Cement & Concrete Composites 35 (2013) 78–88

Contents lists available at SciVerse ScienceDirect

Cement & Concrete Composites

journal homepage: www.elsevier.com/locate/cemconcomp

Life cycle analysis of pavement overlays made with Engineered Cementitious Composites

S.Z. Qian [a,*], V.C. Li [b], H. Zhang [c], G.A. Keoleian [c]

[a] Institute of Highway and Railway Engineering, School of Transportation, Southeast University, Sipailou 2, Nanjing 210096, PR China
[b] The Advanced Civil Engineering Materials Research Laboratory (ACE-MRL), Department of Civil and Environmental Engineering, University of Michigan, Ann Arbor, MI 48109, USA
[c] Center for Sustainable Systems, School of Natural Resources and Environment, University of Michigan, Ann Arbor, MI 48109, USA

ARTICLE INFO

Article history:
Received 29 March 2011
Received in revised form 5 July 2012
Accepted 19 August 2012
Available online 26 August 2012

Keywords:
Sustainable pavement overlay
Engineered Cementitious Composite (ECC)
Ductility
Unbonded concrete overlay
Cracking
Stress concentration

ABSTRACT

While unbonded concrete and hot mixture asphalt overlays have been commonly used for concrete pavement rehabilitation, cracking due to stress concentration still limits the service life of pavement overlays. The use of ductile concrete such as Engineered Cementitious Composite (ECC) should suppress this brittle fracture at the base of the overlay due to existing crack/joint. Therefore, enhancement of long term performance of the overlaid pavements can be expected. Herein we introduce and study the feasibility of this concept via integration of ECC flexural fatigue behavior and finite element analysis for overlaid pavement. The integration results in a service life model for pavement overlays, which was then employed in a life cycle assessment model to reveal the sustainability performance of different overlays. Analysis results suggest that ECC can greatly extend the service life of pavement overlay with less thickness compared with concrete overlay, resulting in a more sustainable overlay.

1. Introduction

Besides hot mixture asphalt (HMA) overlay, unbonded concrete overlay (UBOL) emerged as another rehabilitation method viable for deteriorated rigid pavements [1]. Typical distresses in UBOL include reflective cracking, joint spalling and faulting, fatigue cracking and premature failures due to poor separator layer design, excessive joint spacing and inadequate slab thickness [2]. Among them, cracking due to stress concentration is one of the main factors limiting the service life of overlays [3,4]. Under repeated traffic, daily/seasonal horizontal and differential vertical movements, the preexisting joints/cracks in the substrate concrete tend to penetrate the overlay with flexural, tensile and shear loading. The overlay material responds in a brittle manner under high stress concentration induced by the preexisting joint/crack in the substrate concrete. Several techniques addressing the reflective cracking problem have been attempted, which will be briefly summarized below.

Current techniques may be grouped into at least three broad categories using different approaches to address the reflective cracking problem: concrete slab fracturing [4], stress-relieving (crack relief) interlayer [5,6], and modified overlay [7]. Concrete slab fracturing techniques include rubblization, crack and seat (for plain concrete pavement), and break and seat (for reinforced concrete pavement). By creating small pieces of concrete, the fracturing technique minimizes one of the main mechanisms of reflective cracking, i.e., the horizontal movement of concrete substrate due to temperature and moisture changes [4]. The second broad category involves mainly HMA interlayer. These interlayers are used between the concrete substrate and the concrete UBOL to relieve the stress/strain concentration. The third category, the modified overlay technique, involves addition of fiber reinforcement in the overlay and increasing the overlay thickness. If used appropriately, most of the current techniques can delay the onset of reflective cracking and achieve service life comparable to those of new concrete pavements [1,2].

While the effectiveness of current techniques in addressing reflective cracking has been demonstrated in many cases, there still exist certain areas that can be improved. For instance, a greater overlay thickness is required to compensate for the reduction in structural capacity caused by fracturing the concrete substrate [8]. The addition of asphalt separator layer before placement of unbonded concrete overlay can complicate the construction process. Last but not least, UBOL may involve much shorter joint spacing [9] (e.g. 1.8×1.8 m panels for overlay thickness less than 127 mm) to help minimize curling and warping stresses, which also means significantly increased work for the time sensitive/consuming saw-cutting of the joints. This concludes the introduction to UBOL.

* Corresponding author.
E-mail address: sqian@seu.edu.cn (S.Z. Qian).

0958-9465/$ - see front matter © 2012 Elsevier Ltd. All rights reserved.
http://dx.doi.org/10.1016/j.cemconcomp.2012.08.012

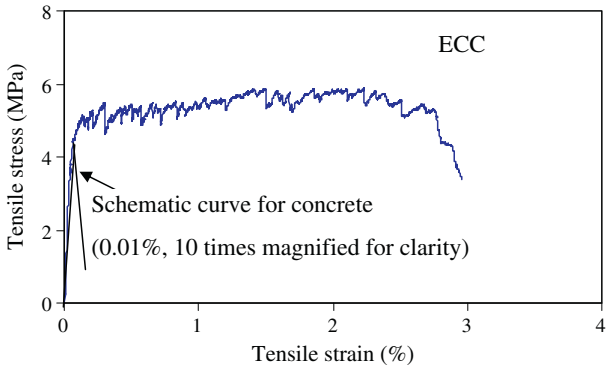

Fig. 1. Typical tensile stress–strain curve of ECC.

To overcome the aforementioned technology challenges, a material-based solution is proposed to resolve the reflective cracking problem. Specifically, in this study, an Engineered Cementitious Composite (ECC) designed for ultra high ductility (Fig. 1) and damage tolerance was considered to replace the HMA/concrete in rigid pavement overlays, aimed at achieving a thin, durable, and cost-effective overlay. This approach exploits the high ductility and damage tolerance of ECC, without relying on concrete slab fracturing or stress relieving interlayers. The ECC overlays can potentially be jointless or have greatly extended joint spacing due to its ductility. Special focus is placed on the high intrinsic material ductility and fatigue resistance for suppressing the reflective cracking in rigid pavement overlays.

ECC is a class of fiber reinforced strain hardening cementitious composites, invented by Li and co-workers based on micromechanics design theory in 1990s [10]. As shown in Fig. 1, above 4.6 MPa, ECC shows a distinct strain-hardening response of about 2.5% strain. In contrast, normal concrete fails at 0.01% strain. ECC attains high ductility with relatively low fiber content (2% or less of short randomly oriented fibers) via systematic tailoring of the fiber, matrix and interface properties, guided by micromechanics principles [11]. An example composition of ECC is shown in Table 1. In this mixture ECC has a compressive strength of 46 MPa, with an elastic modulus of about 20 GPa. Due to its extreme tensile ductility, the flexural strength of ECC can be three to five times compared with its tensile strength [12]. The unit cost of ECC is about three times compared with that of normal concrete [13].

Previous research [14] in using ECC as a repair layer on cracked concrete substrate involved the study of monotonic and/or fatigue behavior of ECC/concrete layered beams (Fig. 2 [14]). The mode of deformation in these specimens provides valuable insights into what might be anticipated in ECC pavement overlays. Highlights of the results of these studies are therefore summarized here. Details of these experiments can be found in the aforementioned references.

The ECC effectively diffused stress concentration by extensive microcrack damage development at the base of the ECC layer (Fig. 2c). By suppressing brittle fracture, the load capacity doubled compared to that of a control specimen with concrete overlay. The corresponding stiffness of the strain-hardening material is reduced by at least two orders of magnitude resulting in a highly non-linear load–deflection response. This automatic response of ECC to high stress-concentration offers the possibility of designing rigid pavement overlays that can effectively eliminate reflective cracking in the overlay. Control studies using common tension-softening FRC in the repair layer show that the system stiffness is maintained until a sudden quasi-brittle spalling crack is formed, causing failure of the FRC overlay. Thus, the automatic stiffness step-down response is unique to materials that strain-harden [14].

2. Overall research framework

The sustainable infrastructure material design framework proposed by Keoleian, Li and coworkers [15] provides a powerful platform for designing material to achieve optimal sustainability for the infrastructure systems. This framework has established the critical connections among material design, structural application, and sustainability modeling. To achieve the goal of sustainable infrastructure, appropriate waste material substitutes are incorporated into the composite material and engineered to achieve desired material composite properties for specific infrastructure applications. Furthermore, a complete life-cycle analysis of the modified infrastructure system is performed to examine the effect of the new green material on the system sustainability. Finally, these results are used as feedback for identifying different substitution materials to further improve system sustainability.

For rigid pavement overlay application, the critical material property considered in this investigation is flexural fatigue response of the ECC material under traffic loads. The shear loading scenario corresponding to differential vertical movements of the slabs across the joints/cracks is not covered in this study. Furthermore, the potential thickness reduction of ECC overlay may be very crucial in enhancing the sustainability of the overlay system. This is because large amount of materials will be utilized in overlay construction. Given the above consideration, this investigation focuses on the examination of the flexural performance of ECC materials under fatigue loading via experiment, along with FEM analysis of ECC overlaid rigid pavement to reveal the influence of overlay thickness on the structural response. From these investigations, a fatigue stress – fatigue life (σ–N) relation and a maximum tensile stress – overlay thickness (σ–H) relation is obtained (Fig. 3). Combining these relations results in an overlay thickness – fatigue life (H–N) relation. This relation provides design guideline for future ECC overlay field application and also facilitates the life cycle analysis of the rigid pavement overlay incorporating ECC materials.

3. Experimental testing on fatigue performance of ECC

3.1. Experimental preparation

Table 1 reveals the mix proportion and mechanical properties of ECC investigated in this study. In addition, concrete from fatigue experiment of Oh [16] was included for comparison. Furthermore, this concrete mixture has a modulus of rupture (MOR, i.e., flexural strength) typically used in pavement [1]. Basic uniaxial tensile, compressive and flexural properties were determined for the ECC at 28 days. Uniaxial tensile testing used coupon plate specimens with dimensions of $304.8 \times 76.2 \times 12.7$ mm. The compressive properties were obtained from cylinder specimens (75 mm by 150 mm in diameter and height, respectively). It should be noted that cracking strength of the concrete was derived from compressive strength based on Mindess et al. [17].

The flexural specimens have a dimension of 356 mm (length), 50 mm (height) and 76 mm (width), with a span between two supports of 305 mm. Four point bending test was conducted at a constant moment span length of 102 mm. The MOR (flexural strength) of ECC and concrete was determined using elastic beam theory. The monotonic test was conducted under displacement control at a rate of 0.5 mm per minute, considering the very large deflection capacity of ECC due to its high tensile ductility. According to Lepech and Li [18], the ECC shows no sign of size effect in flexural test of span up to 2.8 m due to its high ductility, with the crack pattern being the same for thin and thick specimens.

For the fatigue specimens, a static preloading stage (to 0.5 MOR level) and a subsequent fatigue loading stage were applied. The

Table 1
Material properties and mix proportion of ECC and concrete (mix by weight (fiber by volume)).

Material	ε_{tu} (%)	f_{cr} (MPa)	f_{tu} (MPa)	f_c' (MPa)	MOR (MPa)	C	S	CA	FA	W	SP	PVA fiber
ECC	2.5 ± 0.5	4.6 ± 0.3	5.3 ± 0.6	46.0 ± 0.4	10.9 ± 0.9	1.0	0.8	0	1.2	0.59	0.012	0.02
Concrete	0.01	3.2	–	27.0	4.6	–	–	–	–	–	–	–

ε_{tu}: tensile strain capacity; f_{cr}: cracking strength; f_{tu}: ultimate tensile strength; f_c': compressive strength; MOR: modulus of rupture (flexural strength); C: cement; S: sand; CA: coarse aggregate; FA: fly ash; W: water; SP: superplasticizer; PVA fiber: KURALON K-II REC15; hyphen "–": data are not available in the literature.).

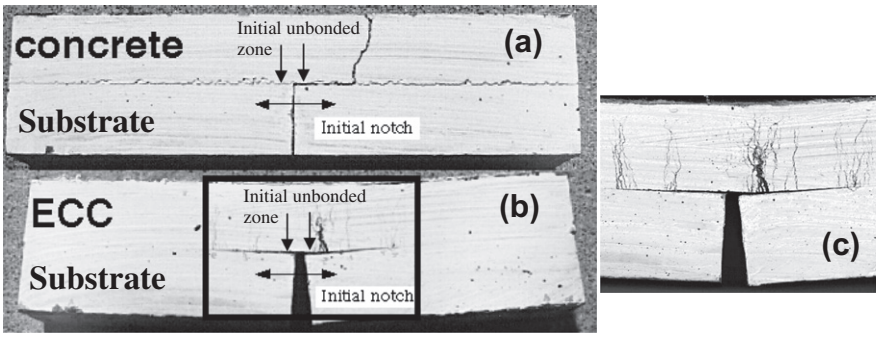

Fig. 2. Comparison of high stress concentration effects on concrete and ECC repair materials, showing (a) brittle fracture in concrete layer, and (b) ductile strain-hardening response in ECC layer. This strain-hardening zone is enlarged in (c) to show microcrack arrests inside the ECC layer. The final failure was due to exhaustion of the flexural capacity of the ECC layer not related to any crack tip effect. Note spalling is suppressed in the ECC.

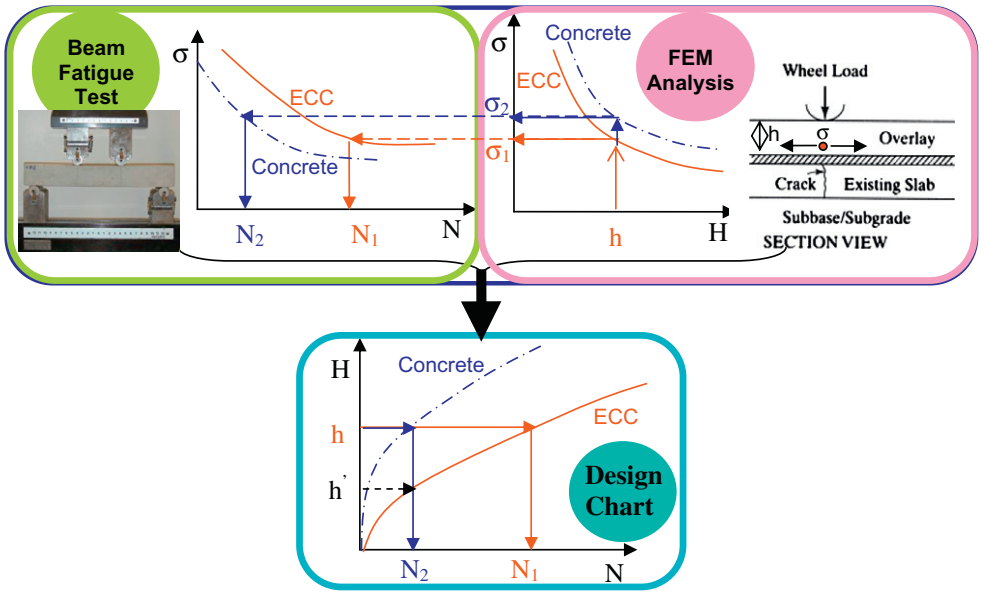

Fig. 3. Integration of FEM analysis and material fatigue test result into design chart (σ critical tensile stress in FEM analysis and maximum fatigue stress in beam fatigue test; H: thickness of overlay; N: fatigue life of overlay).

preloading used displacement control at a rate of 0.5 mm per minute. No microcracks were observed using portable microscope during the preloading stage. After preloading, fatigue cycles began using load control with sinusoidal waveform at a frequency of 8 Hz. The fatigue load ratio (maximum flexural stress, σ_{max} over MOR) was chosen to be 0.7, 0.8 and 0.9. The minimum flexural stress, σ_{min}, was kept to 20% of the maximum flexural stress. The fatigue life (product of frequency and fatigue testing time in seconds) recorded for a given maximum flexural stress was then used to construct the σ–N relation.

3.2. Experimental results

From the monotonic flexural tests, ECC showed an MOR (flexural strength) approximately doubled that of normal concrete, and deformation capacity at least one order of magnitude higher compared with concrete (Fig. 4). This drastic improvement in bending behavior largely comes from the ductile tensile behavior of ECC (Table 1), as found by Maalej and Li [12].

ECC reveal multiple cracking behavior both under monotonic and fatigue loading while concrete always fails by sudden fracture localization, as shown in Fig. 5. As the fatigue stress level decrease, the number of microcracks also decrease in ECC. This observation suggests that when the fatigue load level decrease, it is more difficult for ECC beam to reach saturated multiple cracking since the corresponding tensile stress at the bottom of the beam may be very close to the cracking strength. This phenomenon was also observed by Matsumoto et al. [19]. The number of cracks developed during fatigue loading should influence the ultimate deformation level of the beam at fatigue failure. The more cracks developed during

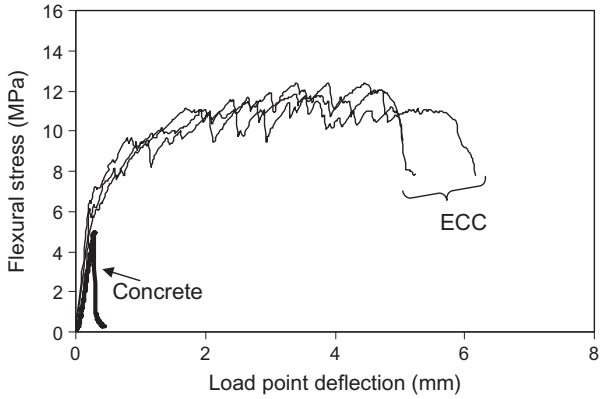

Fig. 4. Flexural stress and load point deflection relation of ECC and concrete.

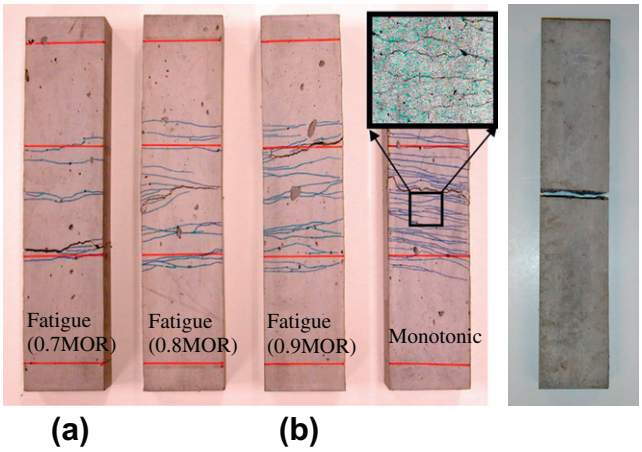

Fig. 5. Crack pattern for (a) ECC specimens under flexural monotonic and fatigue loading; (b) concrete specimen (the microcracks shown in (a) are marked by pen for clarity while actual microcracks before marking are shown in the framed close-up view).

fatigue loading, the larger the deformation achieved at fatigue failure. The fatigue failure is a result of fracture localization of one of many microcracks at the final stage.

Under fatigue loading condition, ECC also shows great enhancement in fatigue stress – fatigue life relation when compared with the concrete. The fatigue stress – fatigue life relation (σ–N relation) is shown in Fig. 6, where concrete from Oh [16] is also shown as reference. As clearly seen, with the same fatigue life, the fatigue stress sustained by the ECC is about twice that of the concrete. It

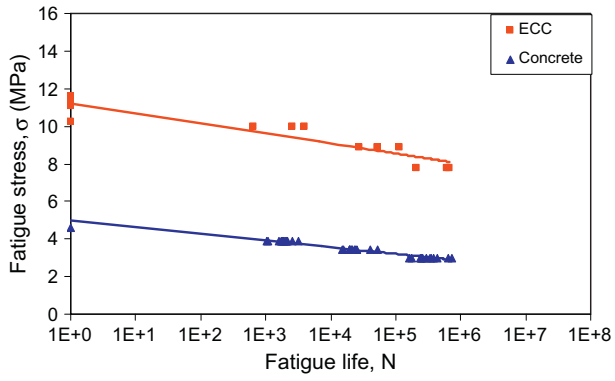

Fig. 6. Fatigue stress–fatigue life relations for ECC and concrete.

is expected therefore, that the introduction of ECC will greatly enhance the service life of concrete pavement overlay. The relatively larger scatter of the ECC compared with those of the concretes in the σ–N plots suggests that the material variation in the ECC could potentially be higher due to fiber non-uniform distribution. This concern should be addressed by more rigorous quality control of ECC or accounted for in an actual pavement overlay design.

In the proposed service life model for pavement overlay in the present feasibility study, only the σ–N regression equations are used for integrating the fatigue test and FEM analysis results, while statistical variation term R^2 is not considered for simplicity. For better prediction of the pavement overlay service life and conducting life cycle analysis on a probabilistic base, it is desirable to incorporate the statistical distribution consideration for σ–N relation. An extensive fatigue experimental program is needed to gain meaningful insight on statistical distribution of fatigue life at different fatigue stress level, which is beyond the scope of this study. Furthermore, the fatigue behavior tested in the laboratory should be calibrated, e.g. via a shift function, for field conditions in the future once ECC overlay is implemented.

4. FEM analysis of pavement overlay

An FEM program specifically developed for pavement application, JSLAB2004 [20] was used for the characterization of critical tensile stress in the ECC overlay under traffic loading. The critical tensile stress is the stress at the bottom of ECC overlay above the underlying crack in concrete substrate under an equivalent single-axis load (ESAL) of 80 kN (Fig. 3). Plate elements based on Kirchhoff's theory (small deformation theory) were used in the analysis with linear elastic behavior assumed. Furthermore, soft elements (element with zero modulus of elasticity) were adopted in the concrete substrate layer to simulate the joint/crack in the existing pavement. The same approach has been adopted by Portland Cement Association (PCA) in an earlier study to develop a design guideline for rigid pavement overlay [3].

JSLAB2004 was specially developed for rigid pavement analysis, and able to analyze jointed pavements under self-weight, traffic and thermal loads. JSLAB2004 can handle up to two layer (either fully bonded or fully debonded) pavement with a limitation of up to nine slabs (three slabs in each direction). The joints can be modeled with uniformly or non-uniformly spaced, circular or non-circular dowels/tie bars, and aggregate interlock. Since the developers had to minimize the use of computer memory, the finite element model of the layered pavement-system (overlay and existing PCC slab) was condensed to just one layer; that is, the stiffness associated with the degrees of freedom of the underlying layer were added to the stiffness matrix of the top layer [21].

A linear elastic behavior is assumed for ECC in the FEM analysis to be consistent with the elastic beam theory assumption used in the calculation of flexural strength in the previous experimental study of σ–N curve of ECC and concrete beams. This simplification should result in a higher computed flexural stress level and therefore a shorter fatigue life, and is therefore conservative in predicting service life of ECC overlay.

4.1. Finite element model for ECC unbonded overlay analysis

JSLAB finite element model for ECC overlay analysis is shown in Fig. 7. In this investigation, the overlay system is simulated by two layers of materials (ECC and concrete) without bond in between. The slab dimension chosen is 6.1 m by 3.66 m. The top and bottom layers are ECC overlay slab and existing concrete slab, respectively. The crack in the existing slab is modeled by soft elements with zero stiffness. The bottom of the slab was constrained vertically by a

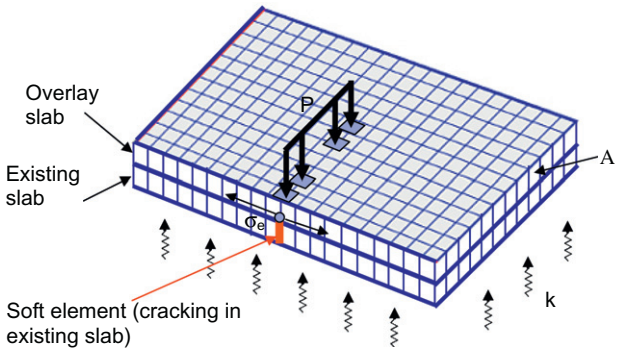

Fig. 7. Finite element model for ECC overlay analysis.

spring at each node with the surface A fixed in both horizontal directions.

The subgrade support was modeled by Winkler foundation, with the force-deflection relationship characterized by an elastic spring [4]. The spring stiffness (k: modulus of subgrade reaction) is varied between 27–81 MN/m^3 (equivalent to 100–300 pci in US customary units), which is directly adopted from Tayabji and Okamoto [3] for comparison purpose. To facilitate future design based on these FEM analysis results, an ESAL of 80 kN was evenly applied over four rectangular areas, each having edge length of 230 mm by 158 mm. The edge of the loading area coincides with the long edge of the overlay slab. The maximum tensile stresses at the bottom of the overlay slab directly underneath the loaded edge thus determined are summarized below.

4.2. Model validation, analysis results and discussions

To validate the modeling, a simple pavement slab was modeled using JSLAB2004 to compare the computed response with the classical Westergaard solution [4] under edge loading. The results from FEM modeling agree well with the Westergaard solution. For more details of the validation, readers are referred to Qian [22].

Furthermore, the FEM model for overlay analysis, a two layered slab system incorporating the effect of crack in concrete substrate (Fig. 7), was also validated with the analysis results from a PCA study [3]. As shown in Fig. 8a and b, comparison between these two studies indicates reasonable agreement (within 6% difference) when the concrete substrate thickness, overlay thickness and modulus of subgrade reaction are varied.

After model validation, the stress concentration effect induced by the pre-existing crack in the substrate concrete on the overlay maximum tensile stress was investigated. Two concrete overlay scenarios, i.e., with and without the existence of a crack in the concrete substrate, were simulated for this purpose. The maximum stress is computed at the base of the ECC overlay on top of the vertical crack in the concrete substrate.

As shown in Fig. 9, the existence of a crack in the substrate concrete does have significant influence on the overlay maximum tensile stress with overlay thickness relation. When the crack is not present, the overlay maximum tensile stress slightly reduces with the decrease of overlay thickness, caused by the shift of load from the overlay to the substrate (the thickness ratio between overlay and substrate reduced from 1:1 to 1:5). In the case of cracked substrate, the overlay maximum tensile stress increases rapidly and non-proportionally with the decrease of the overlay thickness due to the stress concentration effect induced by the existing crack. In the analysis, the modulus of elasticity of concrete substrate (20.7 GPa) is significantly lower compared with that of concrete overlay (24.6 GPa). This is to take into consideration of the reduced

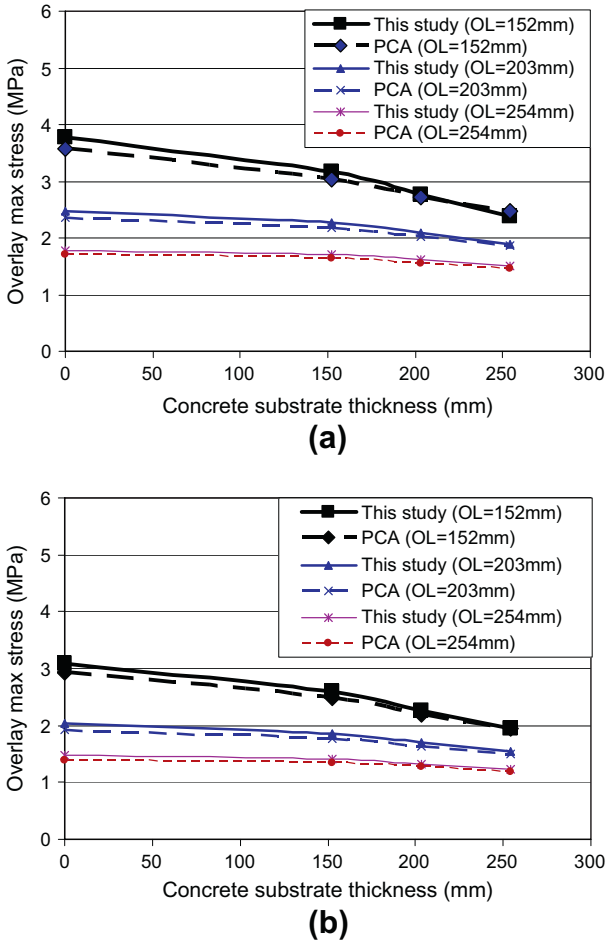

Fig. 8. Comparison of JSLAB analysis with PCA results on the relation of overlay max stress with concrete substrate thickness for (a) modulus of subgrade reaction k = 27.1 MPa/m and (b) k = 81.3 MPa/m (OL = overlay).

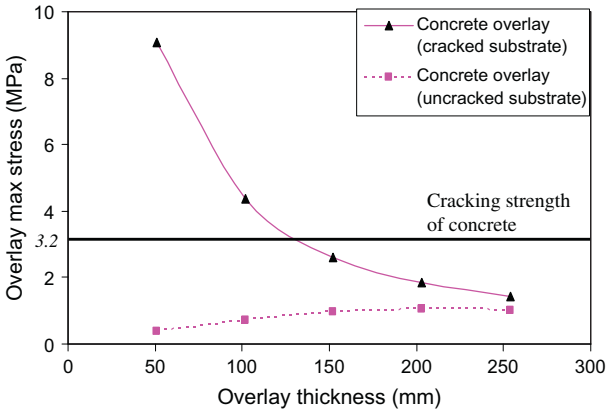

Fig. 9. Effect of substrate pre-existing crack on the overlay bottom maximum tensile stress with thickness relation (concrete substrate thickness = 250 mm; concrete substrate modulus of elasticity = 20.7 GPa and k = 27.1 MPa/m).

quality of concrete substrate, similar to the approach adopted by PCA [3]. It should also be noted that the very high max. tensile stress in cracked substrate case for overlay thickness of 50 mm is due to the linear elastic material assumption adopted in the model. It suggests the propensity of a substrate crack to penetrate the overlay.

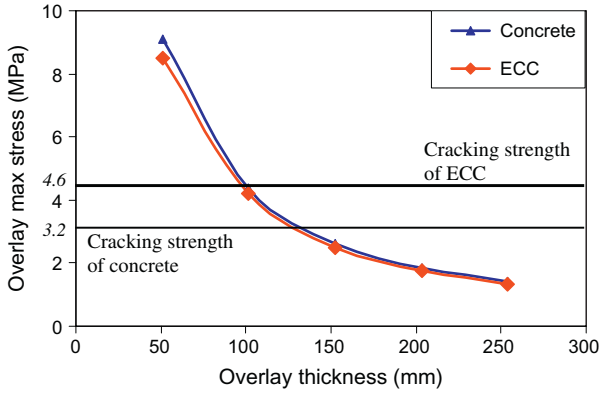

Fig. 10. Overlay slab maximum tensile stress with overlay thickness relation for concrete and ECC (concrete substrate modulus of elasticity = 20.7 GPa and k = 27.1 MPa/m, cracked substrate with thickness of 250 mm assumed).

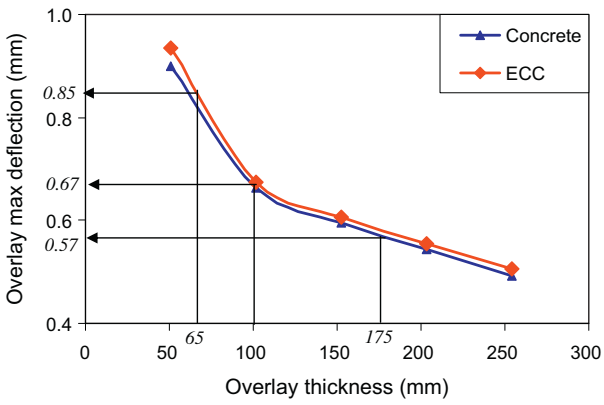

Fig. 11. Overlay slab maximum deflection with overlay thickness relation for concrete and ECC (concrete substrate modulus of elasticity = 20.7 GPa and k = 27.1 MPa/m, cracked substrate with thickness of 250 mm assumed).

The concrete and ECC overlay have modulus of elasticity of 24.6 GPa and 20.7 GPa, respectively. The overlay maximum stress/deflection with overlay thickness relation was shown in Figs. 10 and 11 for concrete and ECC overlay. Due to reduced modulus of elasticity, the maximum tensile stress induced in the ECC overlay is slightly lower compared with that of concrete overlay, while the maximum deflection shows a reverse trend.

Additionally, the effect of the subgrade quality (modulus of subgrade reaction: k) on the ECC overlay maximum tensile stress with overlay thickness relation was investigated (Fig. 12). The results reveal that the maximum tensile stress with overlay thickness relation shifted downward when k increases, with the reduction of maximum tensile stress more pronounced when ECC is relatively thin. This suggests that high quality subgrade is important in the case of ECC overlay application, particularly in the case of thin ECC overlay.

5. Integration of experimental investigation and FEM analysis

Results of the experimental investigation and the FEM analysis were integrated into a deterioration model as schematically illustrated in Fig. 3. The sketched left hand side picture (σ–N curves, Fig. 3) is replaced with the actual experimental results from the flexural fatigue test (Fig. 6). The sketched right hand side picture (σ–H curve, Fig. 3) is now replaced with the results from the FEM analysis (Fig. 10). Assuming certain fatigue life, a corresponding allowable fatigue stress level for each material can be obtained

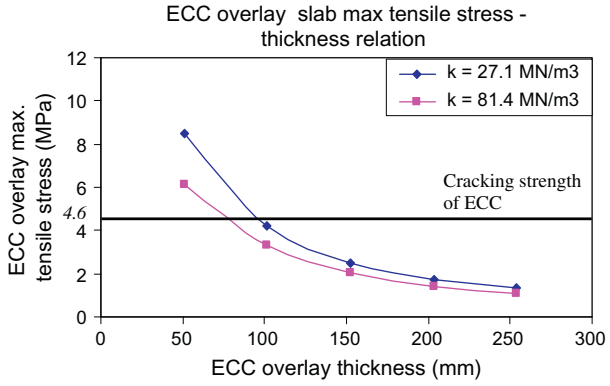

Fig. 12. ECC overlay slab maximum tensile stress with overlay thickness relation for varying modulus of subgrade reaction (concrete substrate thickness = 250 mm; concrete substrate modulus of elasticity = 20.7 GPa).

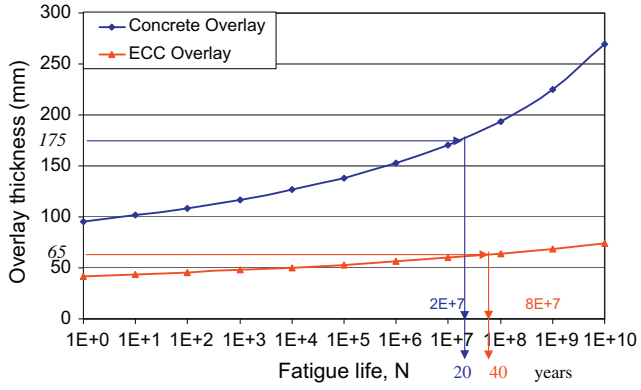

Fig. 13. Service life prediction based on deterioration model for ECC and concrete overlay.

via the σ–N curve. With the same stress level in the overlay slab, the required overlay thickness corresponding to that stress level can then be derived from the σ–H curves. This process can be reversed to find the fatigue life for a material with given overlay thickness.

The integration process resulted in an overlay thickness with fatigue life relation (H–N curve), as shown in Fig. 13. From the figure, it is observed that the concrete overlay requires a thickness about three times that of ECC overlay to achieve a similar fatigue life. This increase in required concrete overlay thickness is mainly driven by the less favorable fatigue behavior of concrete compared to ECC.

Assuming a certain design life for concrete or ECC pavement overlay, the corresponding fatigue life of pavement overlay in terms of equivalent single-axle load (ESAL) can be derived once traffic pattern is specified. With the fatigue life known, the required overlay thickness (concrete or ECC) can be derived from the H–N design curve. The following assumptions are made to facilitate the calculation: design life of 20 and 40 years for concrete and ECC overlay; average daily truck traffic (ADTT) of 5600 (annual average daily traffic (AADT) 70,000 vehicles with 8% heavy duty trucks) and annual growth rate equals to 5%. The total number of ESAL derived is then 2×10^7 and 8×10^7 based on above traffic pattern and design life for concrete and ECC overlay, respectively. It should be noted that the desired fatigue life (total ESALs over design period) increases exponentially with the service life due to the effect of annual growth rate. From the H–N design curves, the required overlay thickness for concrete and ECC is about 175 mm and 65 mm, respectively. The typical range of overlay thickness

used in Michigan is about 150–200 mm with a design life of about 20 years according to MDOT [1]. Hence the model prediction for concrete overlay agrees reasonably well with current practice in Michigan.

While fatigue behavior is very important, the control of overlay maximal deflection is also critical for pavement application. As can be seen in Fig. 11, the maximal deflection is 0.85 mm for ECC overlay of 65 mm thick, which is significantly larger compared with 0.57 mm for concrete overlay of 175 mm thick. According to a FHWA funded study [2], a minimum thickness of 100 mm is needed for unbonded overlay. It is therefore proposed to adopt a thickness of 100 mm instead of 65 mm for ECC overlay to achieve 40 years of service life in the LCA and LCC analysis to be conservative. In this case, the difference of maximal deflection between ECC and concrete overlay is within 0.1 mm, which is expected to be further reduced due to jointless or much extended joint spacing in ECC overlay construction.

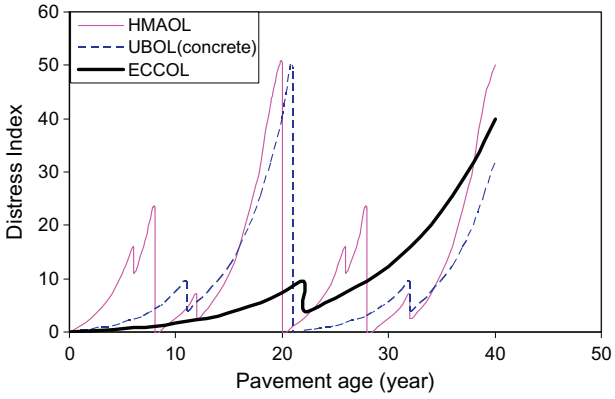

Fig. 15. Distress index and pavement age relation for ECC overlay along with HMA overlay and unbonded concrete overlay (OL = overlay).

6. Service life modeling and sustainability results

6.1. Service life modeling

Given the integrated deterioration model shown above, there is still a need to develop a service life model for ECC in order to facilitate the life cycle assessment (LCA) and life cycle cost (LCC) analysis. MDOT [1] has developed service life models for UBOL and HMA overlay on rubblized concrete (Fig. 14) for LCC use. Before developing a new service life model for ECC, it is useful to gain insights from the existing service life models, such as current MDOT models.

As shown in Fig. 14, an MDOT service life model is developed in the form of distress index (DI) with pavement age relation. The distress index is an index that quantifies the level of distress that exists on a pavement section based on 161 m (0.1 mile) increments. The dominant distress types in DI for composite pavement overlay are transverse crack and transverse joint deterioration [23]. The scale starts at zero and increases numerically as distress level increases (pavement condition worsens). Once the DI reaches 50, the pavement is considered to have exhausted its service life. The service life for UBOL and HMA overlay is 21 and 20 years, respectively.

These maintenance schedules reflect the overall maintenance approach that has been used by MDOT for a specific fix (UBOL and HMA overlay) based on historical maintenance and pavement management records. The only maintenance for the UBOL is during the year 11 after the construction of UBOL. This short term repair for UBOL typically include joint resealing, crack sealing, joint/crack associated concrete patch repairs, and dowel bar retrofit. In case of HMA overlay, there is one major repair – thin HMA overlay and two short-term repairs (typically including crack sealing, chip sealing, etc). In thin HMA overlay repair the top surface (25–50 mm) of the original HMA overlay is usually milled and replaced with new HMA overlay.

From the discussions in the previous section, ECC overlay can sustain a service life of 40 years with a thickness of 100 mm, which is consistent with the ongoing movement toward longer service life requirement. Therefore, as a first attempt, 40 years service life of ECC overlay is used in analysis. Future research can be conducted to determine the optimum service life of ECC overlay from life cycle analysis viewpoint.

Given 40 years service life for ECC overlay with 100 mm thickness, the analysis period for the LCA and LCC is therefore set to be 40 years to coincide with the service life of ECC overlay. In the new DI – age relation (Fig. 15), the DI-age relations for both HMA overlay and UMOL are exactly the same as that shown in Fig. 14 for their service life (20 and 21 years). After that, a new construction of HMA overlay or UBOL is assumed to take place; therefore the DI-age relations for HMA overlay and UBOL repeat themselves

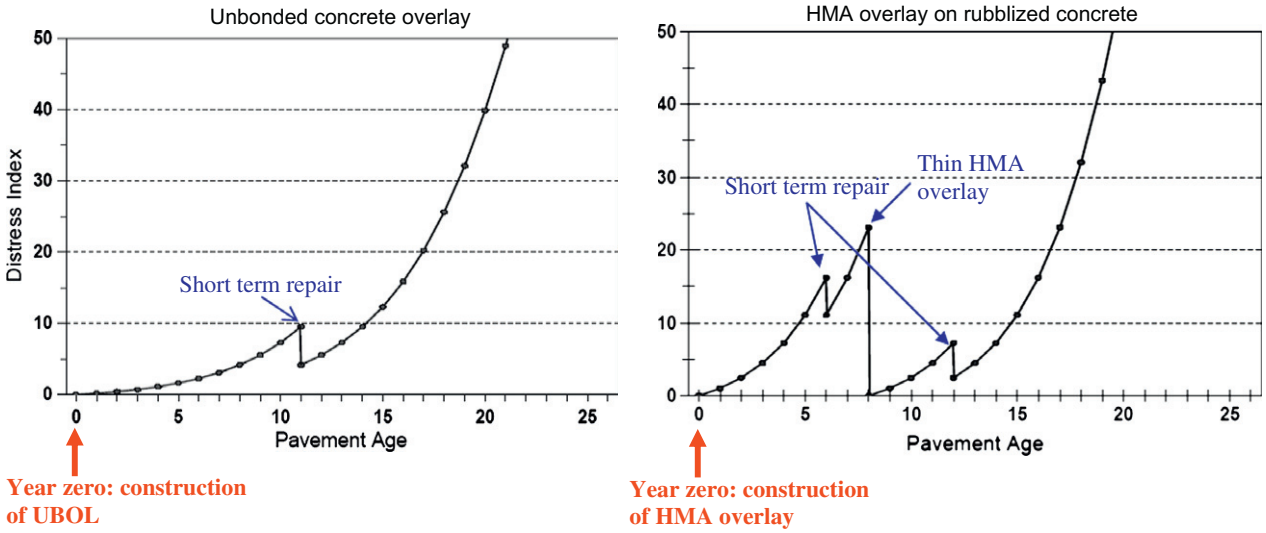

Fig. 14. Distress index and pavement age relations for unbonded concrete overlay and HMA overlay used by MDOT.

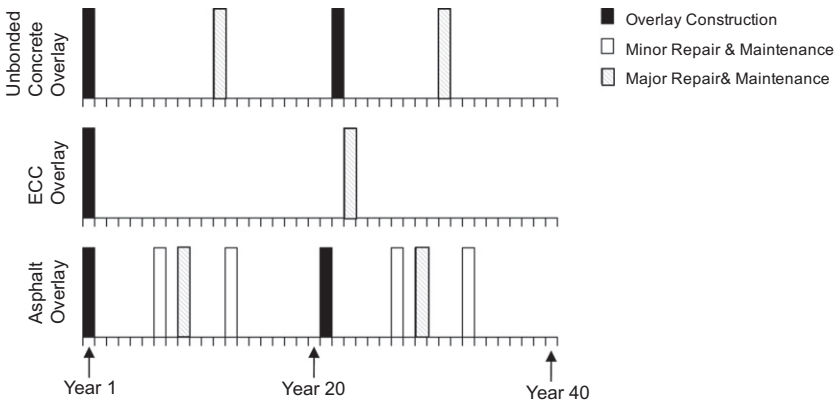

Fig. 16. Timeline and maintenance schedule for different overlay systems.

from year 20 to 40. In case of UBOL, the duplication is not complete since its service life is 21 years. Assuming the increase of DI represents the development of reflective cracking (deterioration mechanism) of UBOL, the DI-age relation for ECC overlay (service life of 40 years) is therefore "stretched" from that of UBOL case (service life of 21 years), meaning the DI of ECC overlay develops at much slow (half of the speed) compared with that of UBOL, considering the service life of UBOL is about half of that of ECC overlay. The corresponding timeline and maintenance schedule for LCA–LCC use are shown in Fig. 16.

In the case of ECC overlay, the current service life model assumes there is only one short term repair event at year 22. This assumption can be warranted if indeed the reflective cracking resistance of ECC is demonstrated and much extended joint spacing can be realized for the ECC overlay, considering short term repair for UBOL includes joint resealing, crack sealing, joint/crack associated concrete patch repairs, and dowel bar retrofit. The reflective cracking resistance mechanism of ECC overlay is reported in Qian [22]. Due to its high tensile ductility capable of accommodating temperature and shrinkage effects, it is very likely that ECC can greatly extend the joint spacing and/or even totally eliminate the expansion joint. A similar idea has been demonstrated in a bridge deck link slab in Michigan [24] and a completely jointless steel/ECC composite bridge deck in Japan [25]. From the above discussions, it seems logical to assume that less frequent repair (once in service life) is needed for ECC overlay.

6.2. LCA–LCC analysis and results

As aforementioned, a life-cycle model was used to evaluate the overall sustainability performance for different overlay systems. This analysis incorporated all components of service life. A schematic of the complete life cycle model is shown in Fig. 17 [26]. Life cycle analysis and modeling work for large scale infrastructures has been proposed and undertaken by Keoleian and coworkers [15,26]. The life cycle assessment includes the following sub-models: material production model, construction model, distribution model, traffic model and fuel economy model.

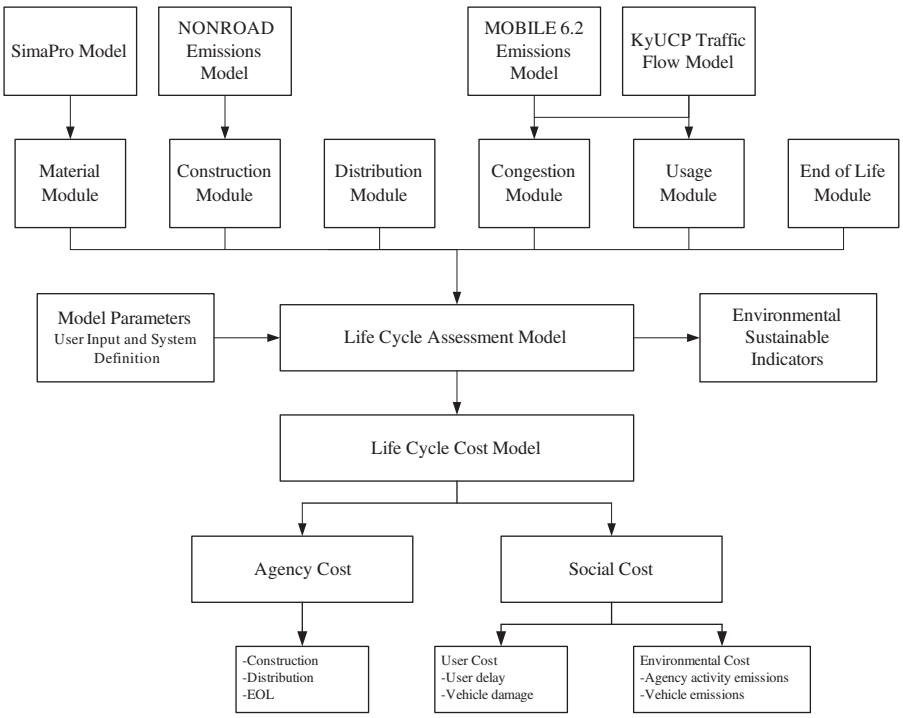

Fig. 17. Life cycle assessment and life cycle cost model.

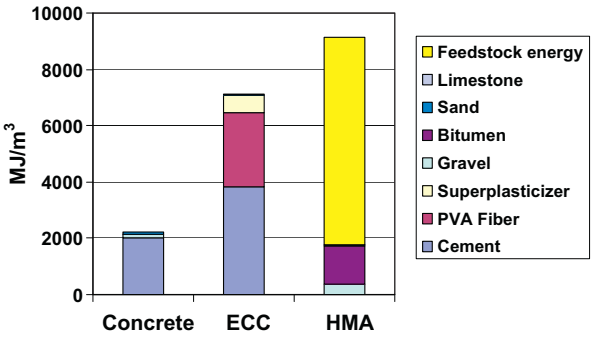

Fig. 18. Energy intensity for different materials.

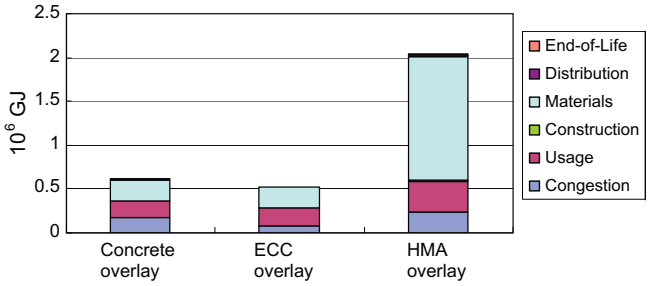

Fig. 19. Total primary energy consumption for different overlay systems.

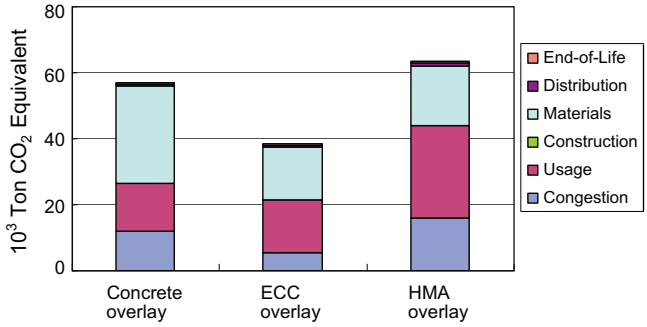

Fig. 20. Global warming index of different overlay systems.

Within the life cycle cost model, economic costs are broken into two major categories, agency and social costs. Agency costs are those borne directly by the government agency (i.e. department of transportation) undertaking the construction work. While some agencies have already incorporated the life cycle concept into decision making processes for their long-term capital investments, such as pavement reconstruction, social costs which are borne by society are typically not accounted for. These include societal pollution damage costs, additional vehicle operational costs, user delay costs, etc. These costs can quickly exceed agency costs over the service life of infrastructure [26]. The details of this LCA–LCC analysis process is beyond the scope of this study and can be found in related literature [26].

Results from the life cycle modeling which examined an existing concrete pavement overlay constructed by MDOT have been detailed by Zhang et al. [26]. Key parameters for this analysis included overlay length 10 km, traffic flow 70,000/day (two ways with four lanes), assumed pavement overlay thickness and service life estimates at given traffic flow from Figs. 11 and 13. The design of overlay structure for HMA overlay and UBOL is from MDOT [1]. Analysis of material production energy impacts reveals that due to the higher cement content and petroleum energy embodied within the PVA fibers, same volume of ECC requires 220% more energy to produce than that for plain concrete (Fig. 18). Similar results are obtained for global warming potential, and other environmental indicators per unit volume of ECC material. While this very high environmental burden is alarming, a complete assessment can only be made by examining the full life cycle of ECC material in a specific infrastructure application, such as an ECC overlay.

Building from ECC overlay deterioration and service life models and combining these with construction data, user data, and national agency and social discount rates, a full assessment of ECC overlay system shows significant benefits for using ECC (Figs. 19 and 20). Due to greatly reduced thickness, much extended service life and less frequent repair events, ECC overlays were found to reduce total primary energy consumption by 75% compared with HMA overlay and slightly less than UBOL even though its material energy intensity is more than three times that of concrete. Similarly, the global warming index is reduced by 32–37% compared with UBOL and HMA overlay. The results suggest that ECC overlay system performs significantly better compared with the other two overlay systems in most of the categories, such as PM_{10}, SO_x, Ammonia, etc. These results suggest that the comparison of sustainability of different materials can only be meaningful from the system viewpoint.

The results from life cycle cost analysis [27] also suggest that, despite of unit material cost as high as three times that of concrete, the ECC overlay reduces total life cycle cost significantly compared with that of UBOL and HMA overlay (Table 2). This is again due to greatly reduced thickness, much extended service life and less frequent repair events. The ECC overlay reduces agency cost, user cost and environmental cost by 38.4%, 39.6% and 22.2% when compared with UBOL, and 58.0%, 55.6% and 36.9% when compared with HMA overlay. Overall, this results in a decrease in life cycle cost from \$72.9 and \$100 million for the UBOL and HMA overlay to \$44.3 million for the ECC overlay, a 39.2% or 55.7% reduction in total costs. While only a small portion of these, approximately 14%, are borne directly by the transportation agency, the reduction in overall costs borne by society as a whole are substantial when using the ECC overlay.

In the current construction practice, the comparison of new material with current materials is often based on dollar per volume basis (e.g \$/m^3), which results in the immediate rejection of new material in most cases. The notion that using a higher unit cost material will be economically disadvantageous may be a misconception, particularly in the case of ECC. As revealed in the previous

Table 2
Comparison of life cycle cost for different overlay systems.

	Concrete overlay	ECC overlay	HMA overlay	ECC overlay cost advantage over concrete overlay (%)	ECC overlay cost advantage over HMA overlay (%)
Agency cost	\$10.1	\$6.22	\$14.8	38.4	58.0
User cost	\$61.9	\$37.4	\$84.2	39.6	55.6
Environmental cost	\$0.9	\$0.7	\$1.11	22.2	36.9
Total cost	\$72.9	\$44.3	\$100	39.2	55.7

Note all units of cost are in millions.

calculation, ECC overlay may outperform concrete UBOL and HMA overlay in terms of life cycle cost and sustainability performance due to great reduction of material usage (via thinner overlay), much extended service life and/or minimized repair events.

7. Conclusions and future works

This paper presents research results on the influence of concrete material ductility and fatigue resistance on rigid pavement overlay performance from a life cycle viewpoint. The overall findings suggest that ECC overlay may be feasible as an alternative technology from those currently used, and shows promise to effectively address the economics, maintenance requirements, and durability performance of rigid pavement overlays. The following specific conclusions can be drawn:

1. ECC is a promising alternative material for a rigid pavement overlay application due to its high fatigue and ductility performance. It was found that ECC can double the service life with greatly reduced thickness compared with that of concrete overlay. The stress concentration induced by the preexisting crack/joint in concrete substrate can be diffused by microcracking process in the ECC overlay and therefore reflective cracking is not expected to occur in the ECC overlay.
2. While the existence of a crack in the concrete substrate does not influence the critical tensile stress for thick overlays significantly, it greatly increases the critical tensile stress for thin overlays due to stress concentration effect. The critical tensile stress in ECC is slightly reduced compared with that in concrete due to lower modulus of elasticity of ECC. High quality subgrade (high modulus of subgrade reaction) can reduce the level of critical tensile stress experienced by ECC.
3. The deterioration and service life models for ECC overlay are successfully developed based on the integration of experimental work and FEM analysis results. These models have proven to be critical in the full life cycle modeling of the ECC overlay system. These models can also be useful for guiding the design of ECC overlays in the future.
4. Results from life cycle analysis suggest that ECC overlay has significant advantages over UBOL and HMA overlay systems due to reduced thickness, extended service life and/or less frequent repair events. A 39.2% or 55.7% reduction in total costs can be achieved when using ECC overlay compared with concrete UBOL or HMA overlay. ECC overlay is found to reduce total primary energy consumption by 75% compared with HMA overlay and greenhouse effect is reduced by 32–37% compared with concrete UBOL and HMA overlay. Despite the much higher material energy intensity and material cost per unit volume (three times compared with those of concrete), ECC overlay performs much better both economically and environmentally. This suggests that a more meaningful comparison between different materials can be achieved through a life cycle modeling of the overlay system that accounts for material performance, volume and costs.

Beyond this feasibility study, significant work is needed so that ECC overlay technology can be ready for deployment in the field. For example experimental study of reflective crack suppression and evaluation of fatigue performance in realistic overlay configurations are essential prior to full scale applications. Furthermore, once the ECC goes into strain-hardening, the effective stiffness of the material will be reduced. The effect on the overlay system needs to be investigated. ECC overlay system response to additional loading types beyond flexure, such as temperature variation and shear loading, also needs to be clarified. The rheology of ECC will likely need to be modified to be compatible with common pavement slip-form construction approach. Finally, validating ECC thickness estimates should be a priority in future work, e.g. through demonstration projects.

Aside from the UBOL application, ECC technology may also be applied in airfield paving or other heavy load pavements. Given the substantially thicker unbonded overlays that are used, a reduction in thickness of overlay would be beneficial economically and environmentally provided the ECC material can withstand the combined mechanical and thermal loads. Ultra-thin whitetopping of roadway pavements is another potential application of interest.

Acknowledgements

The authors would like to acknowledge the financial support from NSF MUSES programs (CMS-0223971 and CMS-0329416), Dr. Mike Lepech for helpful discussions and Dr. Weijun Wang at Federal Highway Administration for help regarding the use of the J-SLAB software. The first author also would like to acknowledge partial financial support from Jiangsu Provincial and Chinese National Natural Science Foundation projects and Jiangsu Top Talents Program in Six Major Disciplines under Grant Nos. BK2010413, 51008071, 51278097, and 2011-JZ-011, respectively for recalculation of FEM results and revision of the manuscript.

References

[1] Michigan DOT. Pavement design and selection manual, michigan department of transportation, Lansing, Michigan; 2005. 65p.
[2] Smith KD, Yu HT, Peshkin DG. Portland cement concrete overlays—state of the technology synthesis. FHWA (IF-02-045); 2002. 192p.
[3] Tayabji SD, Okamoto PA. Thickness design of concrete resurfacing. In: Proc., 3rd Int'l conf on concrete pavement design and rehabilitation. Purdue Univeristy; 1985. p. 367–79.
[4] Huang YH. Pavement analysis and design. 2nd ed. Upper Saddle River, NJ 07458: Pearson Education Inc.; 2004.
[5] Blankenship P, Iker N, Drbohlav J. Interlayer and design considerations to retard reflective cracking. Transport Res Rec 2004;1896:177–86.
[6] Amini F. Potential applications of paving fabrics to reduce reflective cracking. Final report submitted to Mississippi Department of Transportation, Report No. FHWA/MS-DOT-RD-05-174; 2005. 45p.
[7] Hall KT, Correa CE, Simpson AL. Performance of rigid pavement rehabilitation treatments in the SPS-6 experiment. Transp Res Rec 2003;1823:64–72.
[8] Freeman T. Final report evaluation of concrete slab fracturing techniques in mitigating reflective cracking through asphalt overlays. Virginia Transportation Research Council, Charlottesville, Virginia, VTRC 03–R3; 2002. 18p.
[9] American Concrete Pavement Association (ACPA). TB021P-guide to concrete overlay, national concrete pavement technology center. Iowa State University; 2007. 28p.
[10] Li VC, Leung CKY. Steady state and multiple cracking of short random fiber composites. ASCE J Eng Mech 1992;188(11):2246–64.
[11] Li VC, Wang S, Wu C. Tensile strain-hardening behavior of PVA-ECC. ACI Mater J 2001;98(6):483–92.
[12] Maalej M, Li VC. Flexural/tensile strength ratio in engineered cementitious composites. ASCE J Mater Civil Eng 1994;6(4):513–28.
[13] Li VC. High performance fiber reinforced cementitious composites as durable material for concrete structure repair. In: Presentation for ICFRC Int'l conference on fiber composites, high performance concretes, and smart materials, New Delhi, India; 2004.
[14] Zhang J, Li VC. Monotonic and fatigue performance in bending of fiber reinforced engineered cementitious composite in overlay system. J Cement Concr Res 2002;32(3):415–23.
[15] Keoleian GA, Kendall A, Dettling JE, Smith VM, Chandler RF, Lepech MD, et al. Life cycle modeling of concrete bridge design: comparison of ECC link slabs and conventional steel expansion joints. J Infrastruct Syst 2005:51–60.
[16] Oh BH. Fatigue life distributions of concrete for various stress levels. ACI Mater J 1991;88(2):122–8.
[17] Mindess S, Young JF, Darwin D. Concrete. 2nd ed. New Jersey: Prentice Hall 07458; 2003. 644p.
[18] Lepech M, Li VC. Size effect in ECC structural members in flexure. In: Proceedings of FRAMCOS-5, Vail, Colorado, USA; April 2004. p. 1059–66.
[19] Matsumoto T, Suthiwarapirak P, Kanda T. Mechanisms of multiple cracking and fracture of DFRCCs under fatigue flexure. In: Proceedings of the JCI international workshop on Ductile Fiber Reinforced Cementitious Composites (DFRCCs) – application and evaluation (DRFCC-2002), Takayama, Japan; 2002. p. 259–68.

[20] FHWA. JSLAB-2004 user's manual (upgrade supplement). Prepared by Galaxy Scientific Co. for Federal Highway Administration; 2004. 49p.
[21] Carrasco C, Limouee M, Tirado C, Nazarian S, Bendaña J. Development of NYSLAB improved analysis tool for jointed pavement, transportation research record. J Transp Res Board. No. 2227. Washington, DC: Transportation Research Board of the National Academies; 2011. p. 107–15.
[22] Qian S. Influence of concrete material ductility on the behavior of high stress concentration zones. PhD thesis. Ann Arbor: University of Michigan; 2007.
[23] Lee D, Chatti K, Baladi GY. Use of distress and ride quality data to determine roughness thresholds for smoothing pavements as a preventive maintenance action. Transp Res Rec 2002;1816:43–55.
[24] Qian SZ, Lepech MD, Kim YY, Li VC. Introduction of transition zone design for bridge deck link slabs using ductile concrete. ACI Struct J 2009;106(1):96–105.
[25] Li VC. Engineered cementitious composites. In: Proceedings of ConMat'05, Vancouver, Canada; 22–24 August 2005. CD-documents/1-05/SS-GF-01_FP.pdf.
[26] Zhang H, Lepech M, Keoleian G, Qian S, Li VC. Dynamic life cycle modeling of pavement overlay system: capturing the impacts of users, construction, and roadway deterioration. ASCE J Infrastruct Syst 2010;16(4):299–309.
[27] Zhang H, Keoleian GA, Lepech M. An integrated life cycle assessment and life cycle analysis model for pavement overlay systems. In: 1st Int'l symposium on life cycle in civil engineering, Varenna, Lake Como, Italy; 2008. p. 907–12.